

Resonant excitonic emission of a single quantum dot in the Rabi regime

R. Melet,¹ V. Voliotis,^{1,2,*} A. Enderlin,¹ D. Roditchev,¹ X. L. Wang,³ T. Guillet,⁴ and R. Grousson¹

¹*Institut des NanoSciences de Paris, Université Pierre et Marie Curie, CNRS UMR 7588, Campus Bouicaut, 140 Rue de Lourmel, 75015 Paris, France*

²*Université d'Evry Val d'Essonne, Boulevard F. Mitterand, 91025 Evry Cedex, France*

³*Nanotechnology Research Institute, National Institute of Advanced Industrial Science and Technology (AIST), Tsukuba Central 2, Tsukuba 305-8568, Japan*

⁴*Groupe d'Etude des Semiconducteurs, Université Montpellier II, Case Courier 074, 34095 Montpellier Cedex 05, France*

(Received 29 April 2008; revised manuscript received 30 June 2008; published 5 August 2008)

We report on coherent resonant emission of the fundamental exciton state in a single semiconductor GaAs quantum dot. A resonant regime with picosecond laser excitation is realized by embedding the quantum dots in a one-dimensional waveguiding structure. As the pulse intensity is increased, Rabi oscillation is observed up to three periods. The Rabi regime is achieved owing to an enhanced light-matter coupling in the waveguide but with different dynamics with respect to usual cavity quantum electrodynamics. The resonant control of the quantum dot fundamental transition opens new possibilities in quantum state manipulation and quantum optics experiments in condensed-matter physics.

DOI: [10.1103/PhysRevB.78.073301](https://doi.org/10.1103/PhysRevB.78.073301)

PACS number(s): 71.35.-y, 78.67.-n

Manipulation of quantum bits, which are ideally coherently driven two-level systems, is nowadays the subject of an important research effort. In condensed matter, the improvement of growth and integration techniques allows us to think of elementary bricks for quantum computation based on semiconductor quantum dots (QDs). However, interactions between the QD and its environment can cause a severe limitation of quantum coherence.¹ Therefore, in order to take full advantage of the QD state coherence, it is more interesting to manipulate the lowest-lying transition since it is the least interacting with the environment and has the longest coherence time. An important feature of the strong nonlinear interaction between a resonant field and a two-level system is the oscillation of the excited-state population, known as Rabi oscillation (RO).² This is a key experiment for addressing and manipulating a given quantum state. On the other hand, propagation experiments with ultrashort light pulses at resonance with a two-level system can result in coherent phenomena that modify the group velocity of light traveling in the medium, leading to pulse reshaping³ and self-induced transparency,⁴ depending on different regimes of the pulse area. In semiconductor systems, similar coherent effects have been observed, although the physical processes are more complicated because of underlying many-body interactions. RO in quantum wells,⁵ pulse breakup, and self-induced transparency⁶ are some examples of these coherent nonlinearities.

In a one-dimensional (1D) geometry, which is the specific geometry used in the present experiments, if a single two-level atom interacts at resonance with a single confined optical mode, it has been shown⁷ that the system behaves like a highly dispersive medium where photons can be transmitted, reflected, or even stopped. A characteristic feature is the appearance of a frequency “hole” in the absorption of the system. This highly nonlinear behavior depends on the ratio between the radiative cross section of the dipole and the transverse size of the optical mode.⁸ This effect can appear when the light pulses consist of only a few photons or even a single one.

Here, we report an experimental configuration which allows us to perform resonant excitation of the fundamental exciton state in a single QD and an all-optical control in real time of the driven state. Up to now, RO of an excited exciton state in a single QD has been performed.⁹ To our knowledge, resonant *time-resolved emission* of a quantum state in a single QD was not reported because experimentally it is a real challenge to perform excitation and detection at the same wavelength.¹⁰ Only very recently, Muller *et al.*¹¹ reported on resonant experiments on a single QD under cw excitation in a microcavity structure. RO of the fundamental transition in a single QD has recently been observed by means of four-wave mixing¹² or differential transmission¹³ and indirectly by photocurrent measurements.¹⁴ Our basic idea was to combine spatially resolved spectroscopy [micro-photoluminescence (μ PL)] with a 1D waveguiding geometry (Fig. 1). The QDs of interest are embedded in an optical waveguide in which light propagates and interacts with the QDs. The emission of a spatially selected dot is collected in a perpendicular direction, so the scattered laser intensity is

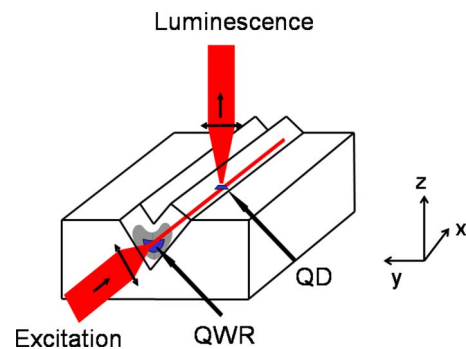


FIG. 1. (Color online) Schematic experimental configuration. The X axis is the free axis of the wire and corresponds to the light propagation direction. The embedded QDs are elongated along the X axis. Y is the light polarization direction and Z is the growth axis. The heart-shaped optical mode and the crescentlike quantum wire are represented in gray and blue colors, respectively.

low compared to the QDs luminescence. We evidenced that in this geometry, the transverse spatial reduction in the optical mode surface leads to an enhancement of the coupling field and the resonant excitation-induced nonlinearities of the excitonic dipole allow RO to occur. The group velocity of the interacting pulses is modified in this highly dispersive medium. This is also discussed in Ref. 7 where a slow light effect is predicted for the case of QDs in a microcavity coupled to a 1D waveguide.

The sample consists of QDs formed naturally by monolayer thickness fluctuations at the interfaces of a GaAs/GaAlAs quantum wire grown by metal organic vapor-phase epitaxy on a V-grooved GaAs substrate. These wires have been extensively studied.¹⁵ The QDs are elongated along the free wire axis with typical lengths from 10 to 100 nm. The number of dots along the wire is thus about 10 per micron as observed by scanning-imaging spectroscopy.¹⁶ The confinement potential along the free wire axis is of the order of magnitude of 10 meV leading to one or two discrete states inside the dots, depending on their size.

In order to form a *monomode* waveguide, the GaAs quantum wire is embedded in AlGaAs layers with different Al concentrations to realize the core and the cladding of the waveguide. Due to the geometry of the structure, the optical modes have a V shape and the polarization of the two fundamental modes is along the Y and Z directions at the center of the waveguide (Fig. 1).¹⁷ The laser beam propagates along the free axis X of the wire and is usually polarized along the Y direction.¹⁸

A specific three optical axis low drift cryostat has been designed for these experiments. A picosecond Ti:sapphire laser source is focused in front of the waveguide by a microscope objective, providing a diffraction limited spatial resolution of the order of 1 μm . The QD luminescence is collected in a perpendicular direction, and a confocal geometry allows us to probe locally about 1 μm^2 . The μPL is analyzed by a spectrometer with a spectral resolution of 40 μeV . A liquid nitrogen-cooled charge-coupled device (CCD) camera or a streak camera with a few picoseconds time resolution are used for spectroscopy or for time-resolved measurements, respectively. To achieve the detection under resonant excitation, the structural quality of the waveguide interfaces is a crucial parameter. Indeed, the inhomogeneities can induce leaks of the laser beam that may completely blur the luminescence signal.¹⁹

The resonant emission of the fundamental exciton state in a QD (Fig. 2) consists of a single Lorentzian line with a FWHM of the order of 100 μeV . The spectral width of the laser pulses is about 500 μeV covering the whole emission line of the exciton. In fact, the μPL linewidth is not related directly to the coherence time of the ground exciton state because the μPL spectrum is the convolution of the spatial response function of the microscope and the homogeneous emission line. The latter can be explained by interaction with acoustic phonons²⁰ and eventually by spectral diffusion effects.^{21,22}

Time-resolved μPL experiments allow us to measure the exciton radiative lifetime. As we have shown, the radiative recombination rate is a linear function of the dot length.²³ Then, we find for the studied QD, with 300 ps radiative

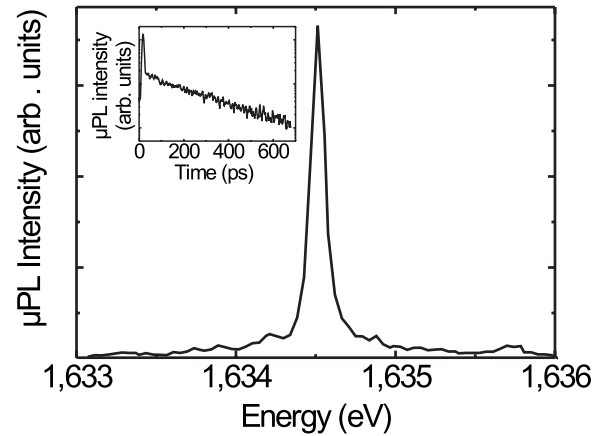


FIG. 2. Resonant emission of a single QD at 10 K and low pump power. Inset: time-resolved μPL excited at resonance. The decay time is in this case $T=300$ ps.

lifetime, a typical length of 40 nm. The dipole moment of the ground exciton transition is $\mu_0=50$ D according to Ref. 24. The obtained value is in agreement with other estimations in similar GaAs QDs and stronger than in the case of InAs self-assembled QDs.^{1,9,25}

Under strong pulsed laser excitation, resonant with a two-level system, RO occurs as a function of the input pulse area (the time-integrated Rabi frequency) $\Theta = \frac{\mu}{\hbar} \int_0^\infty E(t') dt'$, $E(t)$ being the pulse envelope.²⁶ Then, the oscillations observed in the emission intensity scale like \sqrt{I} , where I is the intensity of the field. Figure 3 indeed shows that the intensity of the integrated resonant μPL exhibits periodic RO when plotted as a function of the square root of the laser power. The latter is proportional to the field intensity in the guide, but its absolute value at the position of the QD is difficult to evaluate. We can estimate it however, after correcting for the coupling to the waveguide and other reflection losses. Then $I = \frac{P}{SR\tau}\beta$,

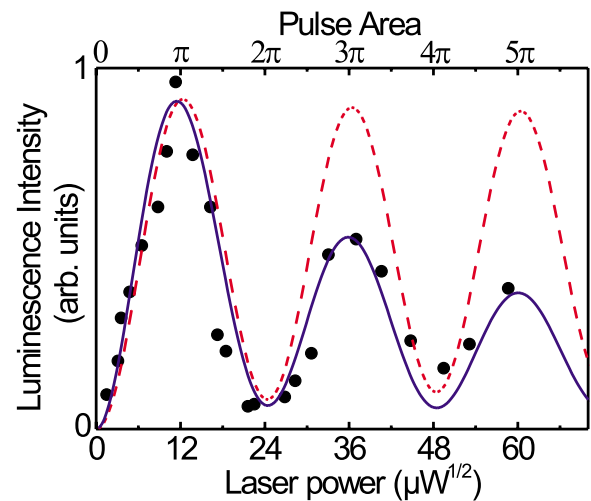


FIG. 3. (Color online) Rabi oscillations obtained from the integrated resonant luminescence (black dots) as a function of the pulse area and the square root of the laser power. The blue (dark gray) solid line and the red (gray) dashed curve represent the calculated time-integrated population of the level with and without damping parameter, respectively.

where P is the mean measured power, S is the surface of the focused laser spot ($1 \mu\text{m}^2$), R is the laser repetition rate (82 MHz), τ is the pulse width (1.5 ps), and β is the correction factor taking into account the geometric losses, such as reflections on the different optical components of the setup. An upper bound for β is estimated to be 10^{-2} . For a π pulse, $P \approx 100 \mu\text{W}$, which is similar to other experimental conditions,^{9,13,14} and the value of the field amplitude at the position of the dot is $E_0 = \sqrt{I/\epsilon_0 c n} = \sqrt{P\beta/SR\tau}$, n being the effective refractive index of the optical mode ($n=3.24$). However, the light-matter interaction between the QD and the optical mode is proportional to the ratio σ_0/A , where σ_0 is the dipole radiative cross section and A is the transverse area of the 1D optical mode.⁸ It is worthwhile noticing that this ratio is also the definition of the so-called ‘‘filling factor,’’ which is introduced in order to explain the global attenuation of the light beam propagating in the waveguide due to the presence of the embedded nanostructure.²⁷ Considering that the QD is a two-level system, the radiative cross section can be calculated by² $\sigma_0 = \frac{\pi\omega_0\mu_0^2 T_2}{3cn\epsilon_0\hbar} = 2 \times 10^{-3} \mu\text{m}^2$. A has been numerically calculated for our specific geometry to be $\sim 0.6 \mu\text{m}^2$. Then the filling factor $F = \sigma_0/A \sim 3 \times 10^{-3}$. Thus the amplitude of the ‘‘effective’’ field interacting with the QD is $E = E_0\sqrt{\sigma_0/A} = E_0\sqrt{F}$.

As the pump intensity is increased, the broad background due to the laser leaks increases linearly and at high intensity it dominates the resonant μPL spectrum. Therefore, in order to consider only the excitonic emission, a background has been subtracted from the μPL spectra. Oscillations up to 5π have been observed in this particular QD corresponding to a pump power of a few milliwatts. Beyond this value it becomes very difficult to distinguish between the QD emission and the scattered laser which becomes one of the main limitations in the manipulation of the state during the coherence regime. Using the optical Bloch equations,²⁸ we can fit the observed RO using a hyperbolic secant pulse. However, this simple two-level model does not predict the observed damping with increasing pulse area (red dashed curve in Fig. 3). Therefore, we introduced a phenomenological intensity dependent damping parameter on the population term to account for the decrease in the oscillation amplitude. In this way, the time-integrated population of the excited state fits quite well the experimental data as shown in Fig. 3 (blue solid line). The set of parameters used for the fit are the population decay time T (measured from the time-resolved luminescence) equal to 300 ps, and the pulse duration of 1.5 ps. Then, two adjustable parameters remain: the intensity-dependent damping parameter and the coherence time T_2 (of the order of 25 ps). This value gives a lower limit for T_2 since the only requirement to fit the data is that the pulse duration must be much smaller than T_2 .

From the optical Bloch equations, the time evolution of the exciton population can also be simulated. The simulations show that as the laser intensity is increased, the decay time decreases. For instance, when the pulse area increases from $\pi/2$ to π , the decay time is reduced by 15%. This was confirmed by the resonant time-resolved μPL experiments where a shortening of the exciton decay time by the same order of magnitude was observed.²⁹ The physical processes

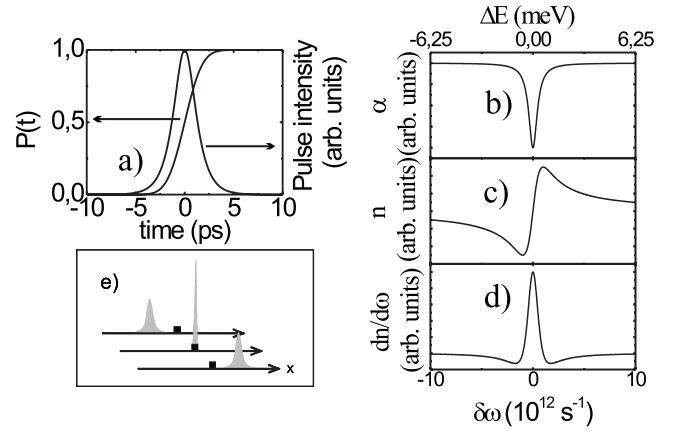


FIG. 4. (a) π -pulse shape and occupation probability $P(t)$ of the excited state. Schematic representation of the frequency dependence of (b) the transparency window, (c) the refractive index, and (d) the dispersion $dn/d\omega$. (e) Schematic spatial compression of the pulse during interaction with the dot (black squares).

underlying this phenomenon can be attributed to nonlinear effects such as two-photon absorption or carrier-carrier scattering.³⁰ A similar Coulomb exciton-exciton scattering mechanism has also been proposed in Ref. 13 to account for the rapid damping of the observed RO.

The value of the dipole moment μ is given by the relation $\Theta \approx 2\tau\frac{\mu E}{\hbar}$. For the set of parameters already used, we find a value of μ about 630 D, which is 13 times higher than the value of μ_0 . Taking into account the error bars on all the parameters (P , β , F , S , and τ), we can estimate that the value of the dipole moment μ ranges between $10\mu_0$ and $300\mu_0$. Intuitively, this is unexpected and a possible explanation is that the dipole interacts with an enhanced coupling field. The origin of this enhancement is likely due to the strong QD-1D optical mode nonlinear coupling that occurs at resonance. In particular, the refractive index varies very strongly at resonance due to a dispersive term $dn/d\omega$ which modifies the group velocity of the propagating pulses.³¹ In the case of large positive dispersion, the group velocity becomes much smaller than the velocity of light in the medium. By Kramers-Kronig relations one finds that when the pulse intensity is increased, a spectral hole emerges in the absorption spectrum at resonance. All these effects are schematically depicted in Fig. 4.

The transparency window around the resonance frequency is the origin for self-induced transparency observed for 2π pulses in atomic gases³ or in semiconductor materials.⁶ One can estimate the value of the group refractive index by assuming that the absorption coefficient of the medium is³² $\alpha(\omega) = \alpha_0 \left(1 - \frac{f}{1 + (\omega - \omega_0)^2/\gamma^2}\right)$, where α_0 is the value of the background absorption, ω is the optical frequency, ω_0 is the resonance frequency, and γ is the linewidth of the transparency window which is of the order of $\sim 1/T$, with T being the total decay time of the two-level system in the 1D waveguide,⁸ which has been measured (see inset of Fig. 2). f is a parameter describing the transparency window, complete transparency is achieved for $f=1$. The refractive index associated to this absorption feature is³² $n(\omega) = n_0 + f \left(\frac{\alpha_0 \lambda}{4\pi}\right) \frac{(\omega - \omega_0)T}{1 + (\omega - \omega_0)^2 T^2}$ and

the group index is at resonance $n_g = n + \omega dn/d\omega \approx \alpha_0 \lambda \omega_0 T / 4\pi = \frac{\alpha_0 L \lambda}{4\pi L} T \omega_0$, where λ is the wavelength in the medium and L is the interaction length equal, in our case, to the QD size. Since the absorption probability $\alpha_0 L$ is given by the ratio σ_0/A , then the maximum value of n_g is $n_g = \frac{\sigma_0 c T}{2\pi n L} \approx 1000$. This means that the pulse is delayed ($v_g = c/n_g$) and experiences a spatial compression during interaction with the dot. This effect is represented schematically in Fig. 4(e). Since the pulse duration remains the same conserving the total energy, the energy density is enhanced by a factor n_g and the dot is coupled to a field with an amplitude n_g times higher. Thus, the strong-coupling regime has been achieved owing to the large oscillator strength of the excitonic transition in interface QDs and to the enhanced interaction between the two-level system and the 1D optical mode.

In summary, resonant luminescence of a coherently driven QD has been directly observed. The 1D waveguiding geom-

etry is a different situation with respect to the cavity geometry where the origin of the strong coupling is the small volume of the discrete cavity modes and the high quality factor. Here, although the QD-waveguide coupling induces relaxation through the mode continuum as discussed in Ref. 8, we believe that the appearance at resonance of spectral filtering in the absorption is the nonlinear effect responsible for strong coupling. Finally, QDs with high radiative cross sections are desirable to enhance the light-matter interaction so that the ratio σ_0/A is the closest to unity as possible. This can be obtained with dots having higher dipole moments or longer coherence times, for instance, with self-assembled QDs.

We thank M. Combescot, F. Dubin, and M. Ravaro for stimulating discussions. This work has been supported by the Region Ile de France (SESAME Grant No. E1751).

*valia.voliotis@insp.jussieu.fr

- ¹Q. Q. Wang, A. Muller, P. Bianucci, E. Rossi, Q. K. Xue, T. Takagahara, C. Piermarocchi, A. H. MacDonald, and C. K. Shih, *Phys. Rev. B* **72**, 035306 (2005).
- ²C. Cohen Tannoudji, J. Dupont-Roc, and G. Grynberg, *Atom-Photon Interactions: Basic Processes and Applications* (Wiley, New York, 1992).
- ³R. E. Slusher and H. M. Gibbs, *Phys. Rev. A* **5**, 1634 (1972).
- ⁴S. L. McCall and E. L. Hahn, *Phys. Rev.* **183**, 457 (1969).
- ⁵S. T. Cundiff *et al.*, *Phys. Rev. Lett.* **73**, 1178 (1994); A. Schülzgen, R. Binder, M. E. Donovan, M. Lindberg, K. Wundke, H. M. Gibbs, G. Khitrova, and N. Peyghambarian, *ibid.* **82**, 2346 (1999).
- ⁶H. Giessen, A. Knorr, S. Haas, S. W. Koch, S. Linden, J. Kuhl, M. Hetterich, M. Grun, and C. Klingshirn, *Phys. Rev. Lett.* **81**, 4260 (1998); M. Jütte *et al.*, *J. Opt. Soc. Am. B* **13**, 1205 (1996); P. C. Ku *et al.*, *Opt. Lett.* **29**, 2291 (2004).
- ⁷A. Auffeves-Garnier, C. Simon, J. M. Gerard, and J. P. Poizat, *Phys. Rev. A* **75**, 053823 (2007).
- ⁸P. Domokos, P. Horak, and H. Ritsch, *Phys. Rev. A* **65**, 033832 (2002).
- ⁹H. Kamada, H. Gotoh, J. Temmyo, T. Takagahara, and H. Ando, *Phys. Rev. Lett.* **87**, 246401 (2001); H. Htoon, T. Takagahara, D. Kulik, O. Baklenov, A. L. Holmes, and C. K. Shih, *ibid.* **88**, 087401 (2002).
- ¹⁰During the submission of our Brief Report, K. Kuroda *et al.*, *Appl. Phys. Lett.* **90**, 051909 (2007), with an oblique incident geometry, performed resonant time-resolved microphotoluminescence.
- ¹¹A. Muller, E. B. Flagg, P. Bianucci, X. Y. Wang, D. G. Deppe, W. Ma, J. Zhang, G. J. Salamo, M. Xiao, and C. K. Shih, *Phys. Rev. Lett.* **99**, 187402 (2007).
- ¹²B. Patton, U. Woggon, and W. Langbein, *Phys. Rev. Lett.* **95**, 266401 (2005).
- ¹³T. H. Stievater, X. Li, D. G. Steel, D. Gammon, D. S. Katzer, D. Park, C. Piermarocchi, and L. J. Sham, *Phys. Rev. Lett.* **87**, 133603 (2001); X. Xu *et al.*, *Science* **317**, 929 (2007).
- ¹⁴S. Stuffer, P. Ester, A. Zrenner, and M. Bichler, *Phys. Rev. B* **72**, 121301(R) (2005).
- ¹⁵J. Bellessa *et al.*, *Appl. Phys. Lett.* **71**, 2481 (1997); T. Guillet, R. Grousson, V. Voliotis, X. L. Wang, and M. Ogura, *Phys. Rev. B* **68**, 045319 (2003).
- ¹⁶T. Guillet *et al.*, *Physica E (Amsterdam)* **17**, 164 (2003).
- ¹⁷D. Crisinel *et al.*, *Opt. Quantum Electron.* **31**, 797 (1999).
- ¹⁸X. L. Wang *et al.*, *J. Cryst. Growth* **171**, 341 (1997).
- ¹⁹R. Melet *et al.*, *Superlattices Microstruct.* **43**, 4771 (2008).
- ²⁰X. L. Wang and V. Voliotis, *J. Appl. Phys.* **99**, 121301 (2006).
- ²¹X. Q. Liu *et al.*, *Appl. Phys. Lett.* **80**, 1894 (2002).
- ²²W. W. Chow, H. C. Schneider, and M. C. Phillips, *Phys. Rev. A* **68**, 053802 (2003).
- ²³J. Bellessa, V. Voliotis, R. Grousson, X. L. Wang, M. Ogura, and H. Matsuhata, *Phys. Rev. B* **58**, 9933 (1998).
- ²⁴L. C. Andreani, G. Panzarini, and J. M. Gerard, *Phys. Rev. B* **60**, 13276 (1999).
- ²⁵J. R. Guest *et al.*, *Phys. Rev. B* **65**, 241310(R) (2002).
- ²⁶L. Allen and J. H. Eberly, *Optical Resonance and Two Level Atoms* (Dover, New York, 1987).
- ²⁷R. Grousson *et al.*, *Semicond. Sci. Technol.* **8**, 1217 (1993).
- ²⁸L. Mandel and E. Wolf, *Optical Coherence and Quantum Optics* (Cambridge University Press, Cambridge, 1995).
- ²⁹R. Melet *et al.*, *Phys. Status Solidi B* **245**, 1098 (2008).
- ³⁰J. Bellessa *et al.*, *Eur. Phys. J. B* **21**, 499 (2001).
- ³¹R. W. Boyd, in *Progress in Optics*, edited by E. Wolf (Elsevier, Amsterdam, 2002), Vol. 43.
- ³²R. W. Boyd, D. J. Gauthier, A. L. Gaeta, and A. E. Willner, *Phys. Rev. A* **71**, 023801 (2005).